Inorg. Chem. **2004**, *43*, 2474–2485

Correlation between ^{19}F Environment and Isotropic Chemical Shift in Barium and Calcium Fluoroaluminates

M. Body,*,†,‡ G. Silly,† C. Legein,‡ and J.-Y. Buzaré†

Laboratoire de Physique de l'Etat Condensé, CNRS UMR 6087, and Laboratoire des Oxydes et Fluorures, CNRS UMR 6010, Institut de Recherche en Ingénierie Moléculaire et Matériaux Fonctionnels, CNRS FR 2575, Université du Maine, Avenue Olivier Messiaen, 72085 Le Mans Cedex 9, France

Received January 9, 2004

High-speed MAS ^{19}F NMR spectra are recorded and reconstructed for 10 compounds from BaF_2–AlF_3 and CaF_2–AlF_3 binary systems which leads to the determination of 77 isotropic ^{19}F chemical shifts in various environments. A first attribution of NMR lines is performed for 8 compounds using a superposition model as initially proposed by B. Bureau et al. The phenomenological parameters of this model are then refined to improve the NMR line assignment. A satisfactory reliability is reached with a root-mean-square (RMS) deviation between calculated and measured values equal to 6 ppm. The refined parameters are then successfully tested on α-$BaCaAlF_7$ whose structure was recently determined. Finally, the isotropic chemical shift ranges are defined for shared, unshared, and "free" fluorine atoms encountered in the investigated binary systems. So, the fluorine surroundings can be deduced from the NMR line positions in compounds whose structure is unknown. Such an approach can also be applied to fluoride glasses.

Introduction

As ^{19}F isotropic chemical shift δ_{iso} is very sensitive to the environment of the fluorine atom, MAS NMR is a powerful structural tool for complex multisite materials. NMR observations of F^- sites in solid materials have become easier with the high spinning speed MAS technology that averages the chemical shift anisotropy and dipole−dipole interactions and reduces spinning sideband overlap. So, ^{19}F NMR spectra obtained with high-speed MAS method can provide important information on environment of fluorine sites for both crystalline and disordered compounds.

Numerous studies[1−8] propose a relation between ^{19}F isotropic chemical shift and local environment of the fluorine atoms.

The approach which is often used is based on the intuitive idea that similar chemical shift values indicate similar structural environments. By comparison with the chemical shift values obtained in basic well-known fluorides, NMR lines of a compound can then be assigned to fluorine sites through their position.[1] When fluorine sites have different multiplicities, relative intensities give also constraints for the line attribution.[2−4] This method has also been applied to studies of glass networks.[2,3] The examination of the influence of the glass composition reinforces the NMR line assignment through their relative intensity variations.[2,3,5,6]

For multicomponent samples, the line assignment is generally not straightforward as fluorine atoms have mixed cationic environments. Stebbins et al.[4,7] proposed an improvement by taking into account the first and second cationic coordination spheres (type and number of cations) for NMR peak attribution. First used in known crystalline compounds, this method led to an empirical calibration of

* To whom correspondence should be addressed. E-mail: monique.body.etu@univ-lemans.fr.

† Laboratoire de Physique de l'Etat Condensé. E-mail: gilles.silly@univ-lemans.fr (G.S.); jean-yves.buzare@univ-lemans.fr (J.-Y.B.).

‡ Laboratoire des Oxydes et Fluorures. E-mail: christophe.legein@univ-lemans.fr (C.L.).

(1) Miller, J. M. *Prog. Nucl. Magn. Reson. Spectrosc.* **1996**, *28*, 255−281.
(2) Stebbins, J. F.; Zeng, Q. *J. Non-Cryst. Solids* **2000**, *262*, 1−5.
(3) Bureau, B.; Silly, G.; Buzaré, J.-Y.; Emery, J.; Legein, C.; Jacoboni, C. *J. Phys.: Condens. Matter* **1997**, *9*, 6719−6736.
(4) Zeng, Q.; Stebbins, J. F. *Am. Mineral.* **2000**, *85*, 863−867.
(5) Bureau, B.; Silly, G.; Buzaré, J.-Y.; Jacoboni, C. *J. Non-Cryst. Solids* **1999**, *258*, 110−118.
(6) Chan, J. C. C.; Eckert, H. *J. Non-Cryst. Solids* **2001**, *284*, 16−21.
(7) Kiczenski, T. J.; Stebbins, J. F. *J. Non-Cryst. Solids* **2002**, *306*, 160−168.
(8) Bureau, B.; Silly, G.; Emery, J.; Buzaré, J.-Y. *Chem. Phys.* **1999**, *249*, 89−104.

10.1021/ic049956r CCC: $27.50
Published on Web 03/19/2004

the chemical shift variation: adding a neighboring cation shifts the line position toward the frequency of the related basic fluoride. The resulting correlation was then applied to analyze NMR spectra for fluoride glasses.

However, with this method insensitive to F−M distances, it is not possible to differentiate between fluorine atoms which have the same number and type of first and second cations. B. Bureau et al.[8] have recently proposed a superposition model on the basis of Ramsey's theory[9] using molecular orbitals obtained by Löwdin's orthogonalization method.[10] The diamagnetic contribution to the ^{19}F isotropic chemical shift, calculated at −127.1 ppm, may be assumed constant in ionic crystalline and disordered fluorides. The paramagnetic part of the ^{19}F shielding in a given environment is simply the sum of the paramagnetic contributions due to all cations in the neighborhood of the considered fluorine atom. Each paramagnetic contribution is a function of the fluorine−cation distance, and only three phenomenological parameters per cation are needed to calculate it. These parameters were deduced for several metal ions from the experimental measurement of δ_{iso} in the corresponding simple fluorides (MF, MF_2, MF_3). The model was satisfactorily tested on fluorides of increasing complexity: fluoroperovskites AMF_3, fluoroaluminates ($KalF_4$, $RbAlF_4$), barium fluorometalates ($BaMgF_4$, $BaZnF_4$, Ba_2ZnF_6), pyrochlore ($CsZnGaF_6$), $PbF_2-M^{II}F_2-M^{III}F_3$ (M^{II} = Ba, Zn; M^{III} = Ga, In) crystalline and glassy phases, and $PbF_2-AF-GaF_3$ (A = Li, Na, K) glasses. The results were found in agreement with the experimental values within a 20% error bar, but at this step, it was not possible to go further because the structures of the lead−fluorogallate crystalline phases are unknown.

Some ab initio calculations were also performed on ^{19}F shielding. Computational studies, using gauge-independent atomic orbitals (GIAO) at the density functional theory (DFT) level, were carried out on a few alkali metal, alkaline-earth metal, and metal fluorides[11−13] with satisfactory results. These calculations involve clusters built-up from the bulk structures. It is quite easy to define such clusters in simple highly symmetric networks, but the task is much more difficult when dealing with low symmetry phases.[14]

The aim of this study is to improve the empirical structure−chemical shift correlation and the superposition model introduced by B. Bureau et al. The samples under study are fluoroaluminates of the BaF_2-AlF_3 and CaF_2-AlF_3 binary systems, which have been chosen because they include numerous crystalline compounds whose structures are known. Moreover, it is possible to obtain glasses in the corresponding ternary. All the studied samples include aluminum atoms, and their crystallographic structures can be described from the AlF_6^{3-} octahedron network. As in lead−fluorogallate compounds, three kinds of fluorine environment can be defined: shared fluorine atoms which bridge two AlF_6^{3-} octahedra, unshared fluorine atoms which belong to only one AlF_6^{3-} octahedron, and "free" fluorine atoms which are not embedded into any AlF_6^{3-} octahedron.[3]

The paper is organized as follows. A first part is devoted to the experimental procedures. In particular, the synthesis conditions of all samples are given since the resulting NMR spectra are very sensitive to the purity and crystalline quality of the samples. All the NMR spectra were recorded using ^{19}F NMR high-speed MAS technique at various spinning rates and numerically reconstructed.

The second part deals with the experimental results and the attribution of the NMR lines. First the structural data are presented in both binary systems, which allow us to perform a partial attribution of the NMR lines considering only the relative intensities. Then, the superposition model is presented, and its application leads to an initial attribution of all the lines in the samples whose structures are known. At last, an improvement of the model leads to modified phenomenological parameters which support new attributions and give a lower RMS deviation between calculated and measured isotropic chemical shifts.

Afterward, our results are compared with previous ones issued from literature, and the evolution of the phenomenological parameters is interpreted. The model with refined parameters is also successfully tested on α-$BaCaAlF_7$ which is a compound of the $BaF_2-CaF_2-AlF_3$ ternary system and whose structure was determined recently.[15] Finally, from the NMR line attribution, the chemical shift ranges for "free", shared, and unshared fluorine atoms are defined. These can be used in studies on disordered materials as glasses or unknown crystalline phases. As an example, fluorine surroundings are deduced from the NMR line positions in β-$CaAlF_5$.

Materials and Methods

1. Synthesis. The crystalline compounds are synthesized as powder by solid-state reaction from mixtures of fluorides AlF_3, CaF_2, and/or BaF_2. All operations of weighing, mixing, and grinding are done under argon atmosphere. Before heating, the mixtures are introduced in Pt tubes sealed under argon atmosphere. The purity and crystallinity of the obtained phases are controlled by X-ray diffraction powder method.

1.1. CaF_2-AlF_3 Binary System. The solid−liquid phase diagram shows two compounds: dimorphic $CaAlF_5$ with a reversible transition α ↔ β around 740 °C, and Ca_2AlF_7.[16,17] These three phases were synthesized for this study.

To obtain the α-$CaAlF_5$ form, a stoichiometric mixture of CaF_2/AlF_3 is heated at 860 °C for 10 days, then slowly cooled to 700 °C, stabilized 2 h at this temperature, and naturally cooled.

β-$CaAlF_5$ is the high temperature phase. It is obtained by heating a stoichiometric mixture of CaF_2/AlF_3 at 860 °C for 10 days followed by quenching in water.[18]

(9) Ramsey, N. F. *Phys. Rev.* **1950**, *78*, 699−703.
(10) Löwdin, P. Ö. *Adv. Phys.* **1956**, *5*, 1−172.
(11) Cai, S.-H.; Chen, Z.; Hu, X.; Wan, H.-L. *Chem. Phys. Lett.* **1999**, *302*, 73−76.
(12) Cai, S.-H.; Chen, Z.; Wan, H.-L. *J. Phys. Chem. A* **2002**, *106*, 1060−1066.
(13) Cai, S.-H.; Chen, Z.; Chen, Z.-W.; Wan, H.-L. *Chem. Phys. Lett.* **2002**, *362*, 13−18.
(14) Silly, G.; Body, M.; Buzaré, J−Y.; Legein, C.; Bureau, B. *C. R. Chim.*, accepted.
(15) Werner, F.; Weil, M. *Acta Crystallogr., Sect. E* **2003**, *59*, i17-i19.
(16) Craig, D.; Brown, J. *J. Am. Ceram. Soc.* **1977**, *60*, 396−398.
(17) Millet, J. P.; Rolin, M. *Rev. Int. Hautes Temp. Refract.* **1981**, *18*, 287−292.
(18) Dance, J.-M.; Videau, J.-J.; Portier, J. *J. Non-Cryst. Solids* **1986**, *86*, 88−93.

Ca_2AlF_7 is obtained by heating a stoichiometric mixture of $2CaF_2/AlF_3$ at 780 °C for a week followed by natural cooling.[19]

1.2. BaF_2-AlF_3 Binary System. The solid−liquid phase diagram shows five compounds: $BaAlF_5$, $Ba_3Al_2F_{12}$, $Ba_5Al_3F_{19}$, Ba_3AlF_9, and Ba_5AlF_{13}.[20] The structures of $Ba_5Al_3F_{19}$ and Ba_5AlF_{13} are unknown so these two compounds are not included in the following study.

Four allotropic varieties of $BaAlF_5$ are known. α-, β-, and γ-forms are obtained from solid-state reactions, with an irreversible transition $\alpha \rightarrow \beta$ at 736 °C, and a reversible transition $\beta \leftrightarrow \gamma$ at 789 °C.[21,22] δ-$BaAlF_5$ crystals were obtained under hydrothermal conditions;[23] however, to our knowledge, it is not possible to synthesize the δ-form from solid-state reaction, so this phase was not included in this study.

α-$BaAlF_5$ is obtained from a stoichiometric mixture of BaF_2/AlF_3 heated at 600 °C for 15 h, and then naturally cooled. β-$BaAlF_5$ is synthesized from the α-form heated for 3 days at 740 °C and naturally cooled. The γ-phase is obtained from the β-form heated 1 day at 850 °C, cooled to 800 °C, stabilized 15 min at this temperature, and then quenched in water.[22]

$Ba_3Al_2F_{12}$ is obtained by heating a stoichiometric mixture of $3BaF_2/2AlF_3$ at 700 °C for 24 h followed by natural cooling.[20]

Ba_3AlF_9 is polymorphic. Different syntheses were performed to obtain the Ia form, but only mixtures were obtained. So, this phase is not included in the following. The Ib form is obtained by heating a stoichiometric mixture of $3BaF_2/AlF_3$ at 830 °C for a week followed by slow cooling at a rate of 1 °C/min. The β-phase is the high temperature form of Ba_3AlF_9: a nonstoichiometric mixture of $2.9BaF_2/AlF_3$ is heated at 880 °C for 14 hours and then quenched in water.[24]

1.3. $BaF_2-CaF_2-AlF_3$ Ternary System. Three polymorphic forms for $BaCaAlF_7$ were reported in the $BaF_2-CaF_2-AlF_3$ ternary system. If the β- and γ-forms were detected by ATD measurement, they were not isolated despite rapid quenching.[25] In contrast, the α-phase was isolated,[25] and its crystallographic structure was recently determined.[15] The α-phase is obtained by heating a stoichiometric mixture of $BaF_2/CaF_2/AlF_3$ at 750 °C for 2 days followed by natural cooling.[25]

2. ^{19}F NMR. All measurements are performed on an Avance 300 Bruker spectrometer using a high-speed CP MAS probe with a 2.5 mm rotor. The external reference chosen for isotropic chemical shift determination is C_6F_6 ($\delta_{iso}(C_6F_6)$ vs $CFCl_3 = -164.2$ ppm).[8] A sequence with a single pulse t_{90} is used (4.1 μs for a magnetic radio frequency field of 61 kHz), followed by the free induction decay acquisition and phase cycling of the receiver. The delay time between two acquisitions is typically 1 s. For each compound, spectra are recorded at different spinning rates between 10 and 35 kHz in order to discriminate isotropic peaks from sidebands, as shown in Figure 1 on β-$CaAlF_5$ spectra.

The chemical shift tensor is described with three parameters: isotropic chemical shift, $\delta_{iso}(ppm) = (\nu - \nu_{ref})10^6/\nu_{ref} = {}^1/_3(\delta_{xx} + \delta_{yy} + \delta_{zz})$; chemical shift anisotropy, $\delta_{aniso}(ppm) = \delta_{zz} - \delta_{iso}$; asymmetry parameter, $\eta = (\delta_{yy} - \delta_{xx})/\delta_{aniso}$. δ_{xx}, δ_{yy}, and δ_{zz} are the eigenvalues of the chemical shift tensor, expressed in its principal axis system.

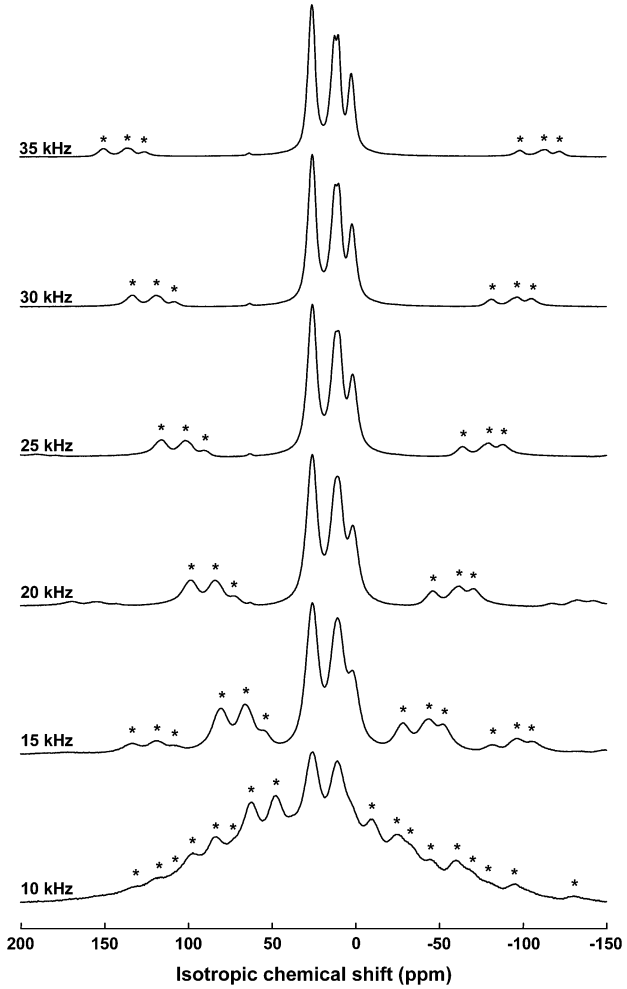

Figure 1. ^{19}F NMR β-$CaAlF_5$ spectrum evolution with the spinning rate frequency. The star symbols indicate the spinning sidebands.

Reconstruction of the spectra is performed with DMFIT[26] software, including spinning sidebands, using four parameters (δ_{iso}, δ_{aniso}, η, and the Gaussian−Lorentzian shape factor) which are supposed to be independent of the spinning rate. On the opposite, the peak intensity and width have to be adjusted for each different spinning speed, since dipolar interaction is not considered in this calculation.

For each compound, δ_{iso}, δ_{aniso}, η, and the Gaussian−Lorentzian shape factor are determined from the reconstruction of the different spinning rate spectra. As expected, high spinning rate spectra give narrower lines and a better precision on δ_{iso} values. At low spinning rates, information on the other components of the chemical shift tensor is obtained through the spinning sideband intensities. Nevertheless, under 15 kHz, the dipolar coupling broadens the NMR peaks too much for a reliable simulation.

Results

1. Structural Data and NMR Spectra. 1.1. CaF_2-AlF_3 Binary System. α-$CaAlF_5$ crystallizes in the monoclinic space group *C2/c* and is built up from isolated infinite chains of AlF_6^{3-} octahedra[27] as shown in Figure 2a. The AlF_6^{3-}

(19) Domesle, R.; Hoppe, R. *Z. Kristallogr.* **1980**, *153*, 317−328.
(20) de Kozak, A.; Samouël, M.; Renaudin, J.; Férey, G. *Z. Anorg. Allg. Chem.* **1992**, *613*, 98−104.
(21) Domesle, R.; Hoppe, R. *Z. Anorg. Allg. Chem.* **1982**, *495*, 16−26.
(22) Le Bail, A.; Férey, G.; Mercier, A.-M.; de Kozak, A.; Samouël, M. *J. Solid State Chem.* **1990**, *89*, 282−291.
(23) Weil, M.; Zobetz, E.; Werner, F.; Kubel, F. *Solid State Sci.* **2001**, *3*, 441−453.
(24) Le Bail, A. *J. Solid State Chem.* **1993**, *103*, 287−291.
(25) Hoffman, M. V. *J. Electrochem. Soc.* **1972**, *119*, 905−909.
(26) Massiot, D.; Fayon, F.; Capron, M.; King, I.; Le Calvé, S.; Alonso, B.; Durand, J.-O.; Bujoli, B.; Gan, Z.; Hoatson, G. *Magn. Reson. Chem.* **2002**, *40*, 70−76.
(27) Hemon, A.; Courbion, G. *Acta Crystallogr., Sect. C* **1991**, *47*, 1302−1303.

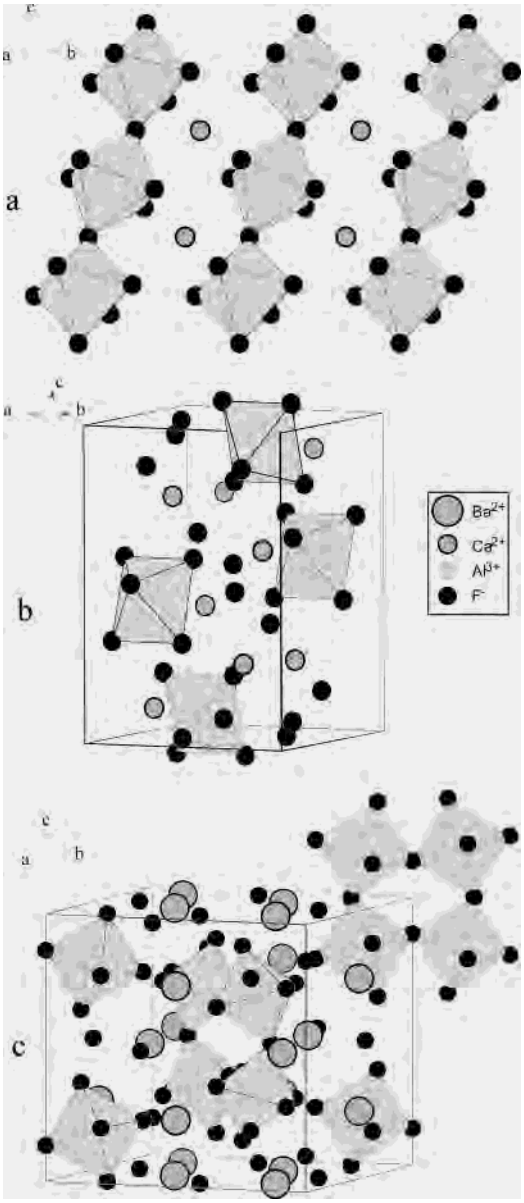

Figure 2. Perspective views of α-$CaAlF_5$ (a), Ca_2AlF_7 (b), and $Ba_3Al_2F_{12}$ (c) structures, exhibiting isolated octahedra, chains of octahedra, and tetrameric groups, respectively.

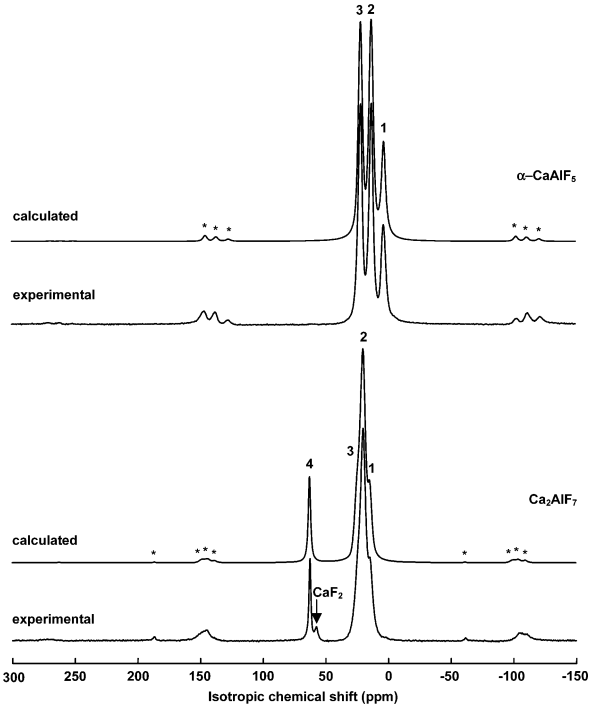

Figure 3. Calculated and experimental ^{19}F MAS NMR spectra of crystalline phases from the CaF_2-AlF_3 binary system at 35 kHz. The spinning sidebands are located under the * symbols.

Table 1. Line Labels, Relative Intensities (%), and $\delta_{iso,exp}$ Values (ppm) As Deduced from NMR Spectrum Simulations, Line Attributions, $\delta_{iso,cal}$, and $\Delta\delta_{iso} = \delta_{iso,exp} - \delta_{iso,cal}$ before and after Refinement of the Superposition Model Parameters for CaF_2-AlF_3 Binary System[a]

line	relative intensity (±2)	$\delta_{iso,exp}$ (±1)	initial parameter sets			final parameter sets		
			site	$\delta_{iso,cal}$	$\Delta\delta_{iso}$	site	$\delta_{iso,cal}$	$\Delta\delta_{iso}$
			α-$CaAlF_5$					
1	20	3	**F 1 (4e, s)**	**−5**	**8**	**F 1**	**5**	**−2**
2	40	13	F 3 (8f, u)	19	−6	**F 3**	**14**	**−1**
3	40	22	F 2 (8f, u)	38	−16	**F 2**	**36**	**−14**
			Ca_2AlF_7					
1	15	15	**F 3 (4c, u)**	**9**	**6**	**F 3**	**3**	**12**
2	57	20	**F 5 (8d, u)**	**25**	**−5**	**F 5**	**22**	**−2**
			F 4 (8d, u)	**28**	**−8**	**F 4**	**24**	**−4**
3	15	25	**F 2 (4c, u)**	**35**	**−10**	**F 2**	**30**	**−5**
4	13	63	**F 1 (4c, f)**	**62**	**1**	**F 1**	**60**	**3**

[a] s, u, and f indicate, respectively, shared, unshared, and "free" fluorine atoms. Unambiguous attributions are in boldface.

octahedra share opposite corners. From the crystallographic data, α-$CaAlF_5$ has three fluorine sites, two with 8f multiplicity and one with 4e multiplicity. So, three isotropic peaks are expected with relative intensities equal to 40%, 40%, and 20%, respectively. The ^{19}F NMR spectrum presented in Figure 3 is in agreement with the spectrum previously recorded by Kiczenski et al.[7] Reconstructions of the experimental spectra at various spinning speeds are obtained with the three expected contributions. Lines 2 (13 ppm) and 3 (22 ppm) have a relative intensity nearly equal to 40%, twice that of line 1 (3 ppm). Consequently, line 1 is attributed to the 4e shared fluorine site and the lines 2 and 3 to the two 8f unshared fluorine sites. Line labels, intensities, and experimental isotropic chemical shifts issued from the simulation of the spectrum recorded at 35 kHz are gathered in Table 1.

Ca_2AlF_7 is described from isolated AlF_6^{3-} octahedra separated from each other by calcium and "free" fluorine ions,[19] as shown in Figure 2b. Ca_2AlF_7 adopts the *Pnma* space group and has three 4c and two 8d fluorine sites. So five peaks are expected: three with a relative intensity equal to 14.3% and two equal to 28.6%. The recorded spectrum, presented in Figure 3, has two peaks and is in agreement with the results of Kiczenski et al.[7] Reconstructions of experimental spectra at various spinning speeds are obtained with four contributions, and the data issued from the simulation of the spectrum recorded at 35 kHz (line labels, intensities and δ_{iso} values) are collected in Table 1. Three lines, 1 (15 ppm), 2 (20 ppm), and 3 (25 ppm), are needed to simulate the most intense peak. Lines 1, 3, and 4 (63 ppm) have nearly the same relative intensity about 14% while line 2 relative intensity is four times larger. Consequently, lines

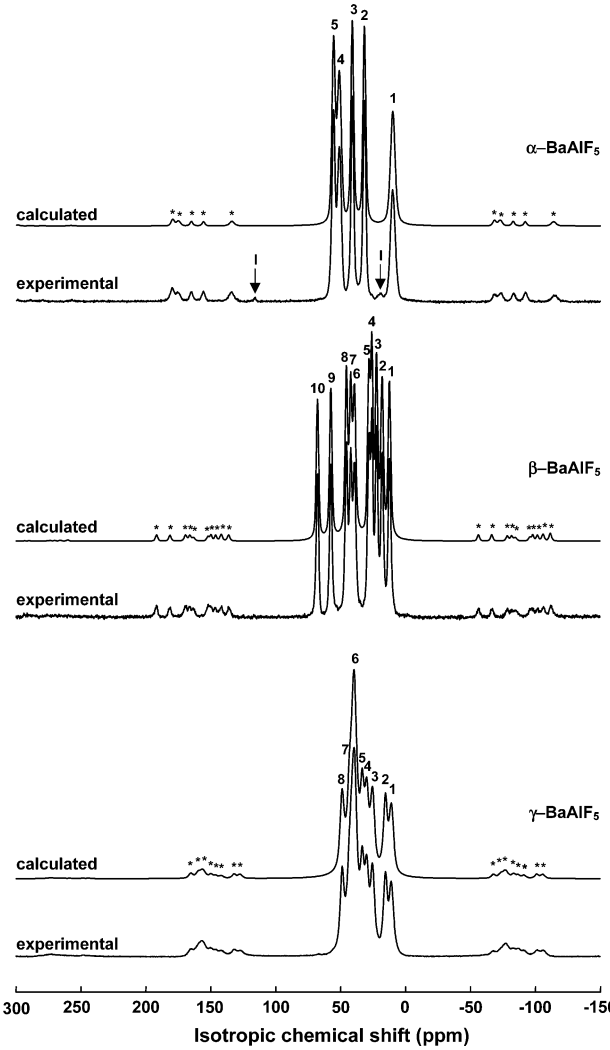

Figure 4. Calculated and experimental ^{19}F MAS NMR spectra of three $BaAlF_5$ allotropic forms at 35 kHz. The spinning sidebands are located under the * symbols. The "I" labels indicate lines belonging to $Ba_3Al_2F_{12}$ present as an impurity in α-$BaAlF_5$.

1, 3, and 4 are attributed to the 4c sites which may correspond to unshared or "free" fluorine atoms and line 2 to the two 8d unshared fluorine sites.

1.2. BaF_2-AlF_3 Binary System. α-$BaAlF_5$, *β*-$BaAlF_5$, and *γ*-$BaAlF_5$ have similar structures built up from isolated chains of AlF_6^{3-} octahedra sharing neighboring corners.[21,22]

α-$BaAlF_5$ crystallizes in the $P2_12_12_1$ space group and has five fluorine sites with the same 4a multiplicity.[21] So, five peaks with the same relative intensity are expected. The ^{19}F NMR spectrum, shown in Figure 4, presents seven peaks. The splitting between peaks 4 and 5 is visible only for spinning rates higher than 15 kHz. The simulation indicates that the relative intensities for lines 1−5 are nearly equal to 20% as expected. Consequently, they are attributed to α-$BaAlF_5$, which is in agreement with the results of Kiczenski et al.[7] Each of these lines can be attributed to one fluorine site. Line labels, intensities, and experimental isotropic chemical shifts issued from the simulation of the spectrum recorded at 35 kHz are collected in Table 2. Two other peaks, labeled "I", with very low relative intensities are measured at 21 and 117 ppm. A comparison with tabulated data for the other phases of this binary system indicates that these two peaks are due to the $Ba_3Al_2F_{12}$ compound, present as an impurity in α-$BaAlF_5$.

Table 2. Line Labels, Relative Intensities (%), and $\delta_{iso,exp}$ Values (ppm) As Deduced from NMR Spectrum Simulations, Line Attributions, $\delta_{iso,cal}$, and $\Delta\delta_{iso} = \delta_{iso,exp} - \delta_{iso,cal}$ before and after Refinement of the Superposition Model Parameters for $BaAlF_5$ Phases[a]

	relative intensity	$\delta_{iso,exp}$	initial parameter sets			final parameter sets		
line	(±2)	(±1)	site	$\delta_{iso,cal}$	$\Delta\delta_{iso}$	site	$\delta_{iso,cal}$	$\Delta\delta_{iso}$
			α-$BaAlF_5$					
1	19	10	**F 5 (4a, s)**	**3**	**7**	**F 5**	**11**	**−1**
2	20	32	F 4 (4a, u)	56	−24	F 4	38	−6
3	20	41	F 3 (4a, u)	63	−22	F 3	39	2
4	20	51	F 1 (4a, u)	88	−37	F 1	49	2
5	21	56	F 2 (4a, u)	91	−35	F 2	55	1
			β-$BaAlF_5$					
1	11	12	F 1 (4e, s)	0	12	F 1	13	−1
2	10	18	F 5 (4e, s)	8	10	F 5	14	4
3	12	22	F 2 (4e, u)	40	−18	F 2	25	−3
4	9	26	F 10 (4e, u)	41	−15	F 10	27	−1
5	10	28	F 6 (4e, u)	55	−27	F 9	34	−6
6	9	39	F 7 (4e, u)	62	−23	F 7	37	2
7	11	42	F 9 (4e, u)	68	−26	F 6	38	4
8	10	46	F 4 (4e, u)	76	−30	F 4	40	6
9	10	58	F 3 (4e, u)	76	−18	**F 3**	**47**	**11**
10	9	68	F 8 (4e, u)	98	−30	**F 8**	**54**	**14**
			γ-$BaAlF_5$					
1	9	17	F 10 (2a, s)	5	12	F 10	20	−3
2	10	21	F 9 (2a, s)	17	4	F 6	22	−1
3	9	30	F 6 (2a, u)	46	−16	F 9	25	5
4	10	34	F 4 (2a, u)	47	−13	F 4	30	4
5	10	37	F 7 (2a, u)	52	−15	F 8	31	6
6	31	43	F 5 (2a, u)	55	−12	F 7	33	10
			F 8 (2a, u)	59	−16	F 1	35	8
			F 2 (2a, u)	61	−18	F 5	36	7
7	12	46	F 1 (2a, u)	61	−15	F 2	41	5
8	9	51	F 3 (2a, u)	84	−33	**F 3**	**49**	**2**

[a] s, u, and f indicate, respectively, shared, unshared, and "free" fluorine atoms. Unambiguous attributions are in boldface.

β-$BaAlF_5$ which crystallizes in the monoclinic $P2_1/n$ space group has ten distinct positions of fluorine atoms with the same 4e multiplicity.[22] Ten peaks are observed in the experimental spectrum (Figure 4) and have the same relative intensity nearly equal to 10% in the spectrum simulations. Consequently, each peak may be attributed to one fluorine site. The data issued from the simulation of the spectrum recorded at 35 kHz (line labels, intensities, and δ_{iso} values) are collected in Table 2.

γ-$BaAlF_5$ crystallizes in the $P2_1$ space group, and its structure exhibits ten fluorine sites with 2a multiplicity.[22] So, the experimental spectra are expected to show ten peaks. Though the recorded spectrum, shown in Figure 4, presents only seven peaks, eight contributions are needed for the simulation: the most intense peak presents a shoulder, and two lines are necessary to give a fine reconstruction of its shape. Line labels, intensities, and experimental isotropic chemical shifts issued from the simulation of the spectrum recorded at 35 kHz are summarized in Table 2. Of the eight lines, seven have relative intensities nearly about 10%, so each one corresponds to one 2a fluorine site. The relative intensity of line 6 is nearly equal to 30% which corresponds to the superimposition of three other 2a fluorine contributions.

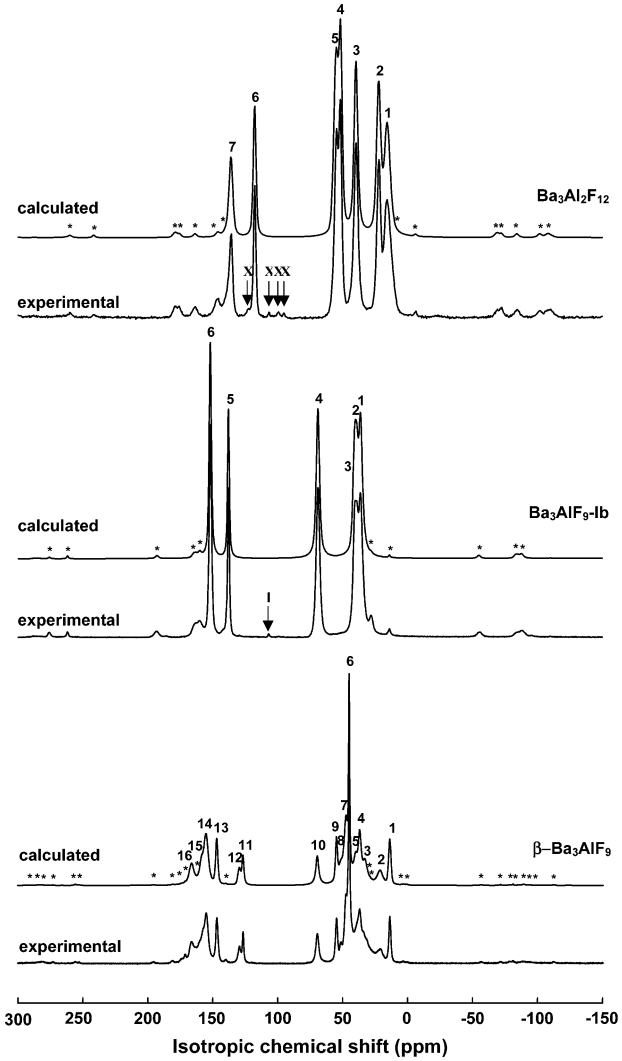

Figure 5. Calculated and experimental ^{19}F MAS NMR spectra of crystalline phases from the BaF_2-AlF_3 binary system at 35 kHz. The spinning sidebands are located under the * symbols. The "I" label represents Ba_5AlF_{13} lines present as an impurity in the Ba_3AlF_9-Ib sample, and "X" labels indicate lines belonging to unknown phase(s) present as impurity in the $Ba_3Al_2F_{12}$ sample.

The structure of $Ba_3Al_2F_{12}$ is built up from rings formed by four AlF_6^{3-} octahedra sharing neighboring corners.[28] These tetrameric groups are separated from each other by barium and "free" fluorine ions as shown in Figure 2c. $Ba_3Al_2F_{12}$ crystallizes in the *Pnnm* space group with eight distinct positions of fluorine atoms in the structure: four with 4g multiplicity and four with 8h multiplicity. So, eight peaks are awaited on experimental spectra, four with relative intensities equal to 8.3% and four equal to 16.7%. However, the recorded spectrum, presented in Figure 5, has eleven peaks, and the discrimination of peaks 4 and 5 is possible only for spinning rates equal to 25 kHz or higher. The simulation indicates that the relative intensities for lines 1−7 are equal to or larger than 8.3%, so they are attributed to $Ba_3Al_2F_{12}$ compound, whereas the relative intensities of the four peaks labeled "X" are lower than 1%. These last four peaks have their chemical shift values measured at 95, 100, 107, and 123 ppm, respectively; however, comparison with tabulated data for the other phases of this binary system does not permit us to identify the impurity, nor does the powder XRD diagram. The seven lines assigned to $Ba_3Al_2F_{12}$, their intensities, and δ_{iso} values measured at 35 kHz are summarized in Table 3. Lines 6 (117 ppm) and 7 (135 ppm) have their relative intensities calculated from simulation around the expected 8.3% value, so they are both attributed to either two 4g shared or "free" fluorine sites. The five other peaks have relative intensities calculated around 16.7%. Consequently, four of them are assigned to the four 8h unshared fluorine sites, and one is attributed to two of the remaining 4g fluorine sites.

Ba_3AlF_9-Ib and β-Ba_3AlF_9 have similar structures: isolated AlF_6^{3-} octahedra separated from each other by barium and "free" fluorine atoms.[24,29]

Ba_3AlF_9-Ib adopts the *Pnma* space group, and its structure exhibits six fluorine sites, three with 4c multiplicity and three with 8d multiplicity. Six peaks are expected on the experi-

Table 3. Line Labels, Relative Intensities (%), and $\delta_{iso,exp}$ Values (ppm) As Deduced from NMR Spectrum Simulations, Line Attributions, $\delta_{iso,cal}$, and $\Delta\delta_{iso} = \delta_{iso,exp} - \delta_{iso,cal}$ before and after Refinement of the Superposition Model Parameters for $Ba_3Al_2F_{12}$, Ba_3AlF_9-Ib, and β-Ba_3AlF_9[a]

	relative		initial parameter sets			final parameter sets		
line	intensity (±2)	$\delta_{iso,exp}$ (±1)	site	$\delta_{iso,cal}$	$\Delta\delta_{iso}$	site	$\delta_{iso,cal}$	$\Delta\delta_{iso}$
			$Ba_3Al_2F_{12}$					
1	17	15	F 1 (4g, s)	8	7	F 1	14	1
			F 2 (4g, s)	10	5	F 2	21	−6
2	16	21	F 8 (8h, u)	32	−11	F 8	18	3
3	17	39	F 7 (8h, u)	81	−42	F 7	52	−13
4	16	50	F 6 (8h, u)	88	−38	F 6	58	−8
5	18	54	F 5 (8h, u)	102	−48	**F 5**	**66**	**−12**
6	9	117	**F 4 (4g, f)**	**98**	**19**	**F 4**	**121**	**−4**
7	8	135	**F 3 (4g, f)**	**141**	**−6**	**F 3**	**145**	**−10**
			Ba_3AlF_9-Ib					
1	23	36	**F 6 (8d, u)**	**52**	**−16**	**F 6**	**29**	**7**
2	12	39	F 1 (4c, u)	51	−12	**F 1**	**33**	**6**
3	12	41	F 2 (4c, u)	64	−23	**F 2**	**43**	**−2**
4	22	69	**F 5 (8d, u)**	**114**	**−45**	**F 5**	**75**	**−6**
5	11	138	**F 3 (4c, f)**	**114**	**24**	**F 3**	**120**	**18**
6	21	152	**F 4 (8d, f)**	**163**	**−11**	**F 4**	**159**	**−7**
			β-Ba_3AlF_9					
1	5	19	F 7 (4c, u)	23	−4	**F 7**	**19**	**0**
2	4	26	F 1 (4c, u)	38	−12	**F 1**	**27**	**−1**
3	7	37	F 4 (4c, u)	60	−23	F 4	37	0
4	7	41	F 10 (4c, u)	64	−23	F 10	43	−2
5	7	44	F 11 (4c, u)	70	−26	F 8	45	−1
6	13	49	F 8 (4c, u)	73	−24	F 6	46	3
			F 6 (4c, u)	73	−24	F 11	47	2
7	11	52	F 12 (4c, u)	87	−35	F 9	50	2
			F 9 (4c, u)	91	−39	F 12	56	−4
8	4	56	F 2 (4c, u)	98	−42	F 2	64	−8
9	4	59	F 5 (4c, u)	104	−45	F 5	66	−7
10	6	73	F 3 (4c, u)	135	−62	**F 3**	**82**	**−9**
11	3	130	**F 19 (2a, f)**	**116**	**14**	**F 19**	**126**	**4**
12	2	132	**F 18 (2b, f)**	**179**	**−47**	**F 18**	**144**	**−12**
13	5	149	F 13 (4c, f)	149	0	**F 17**	**143**	**6**
14	12	158	F 14 (4c, f)	158	0	F 13	151	7
			F 15 (4c, f)	173	−15	F 14	156	2
15	5	161	F 16 (4c, f)	194	−33	F 15	164	−3
16	5	169	F 17 (4c, f)	246	−77	F 16	166	3

[a] s, u, and f indicate, respectively, shared, unshared, and "free" fluorine atoms. Unambiguous attributions are in boldface.

(28) Domesle, R.; Hoppe, R. *Z. Anorg. Allg. Chem.* **1982**, *495*, 27−38.

(29) Renaudin, J.; Férey, G.; de Kozak, A.; Samouël, M. *Eur. J. Solid State Inorg. Chem.* **1991**, *28*, 373−381.

mental spectra, with relative intensities equal to 11.1% and 22.2%, respectively. The recorded spectrum, presented in Figure 5, shows seven peaks. The spectrum reconstruction indicates that the relative intensities for lines 1−6 are equal to or larger than 10%, so they are attributed to Ba_3AlF_9-Ib compound, whereas the relative intensity of the remaining peak is lower than 1%. This last peak, measured at 107 ppm, is attributed from powder XRD to Ba_5AlF_{13} present as an impurity. The six remaining lines issued from the simulation of the spectrum recorded at 35 kHz, their intensities, and δ_{iso} values are summarized in Table 3. Lines 1 (36 ppm), 4 (69 ppm), and 6 (152 ppm) which have the highest relative intensities are assigned to the 8d fluorine sites. Lines 2 (39 ppm), 3 (41 ppm), and 5 (138 ppm) with relative intensities about 11% are attributed to the 4c fluorine sites.

β-Ba_3AlF_9 which crystallizes in the *Pnc*2 space group has nineteen fluorine sites: seventeen with 4c multiplicity, one with 2a multiplicity, and one with 2b multiplicity. So, the experimental spectra should include nineteen peaks, seventeen with relative intensities equal to 5.6% and two with relative intensities equal to 2.8%. More accurate information is obtained at 35 kHz spinning rate. Though the recorded spectrum, shown in Figure 5, presents only twelve peaks, a satisfactory reconstruction was obtained with no less than sixteen contributions. Line labels, intensities, and δ_{iso} values issued from the simulation of the spectrum recorded at 35 kHz are collected in Table 3. Lines 11 (130 ppm) and 12 (132 ppm) which have the lowest relative intensities, calculated around 2.5%, are attributed to the 2a and 2b "free" fluorine sites. Lines 6, 7, and 14 have their relative intensities twice larger than expected: about 11%. Each is assigned to two 4c fluorine sites. The other lines have relative intensities around 5.6%, and each one is attributed to one 4c fluorine site. The limits of the method of line attributions based on relative intensities are reached with this compound, as the difference between the line relative intensities expected for 2 and 4 multiplicity sites is 2.8% when the uncertainty on the calculated values is of ±2%.

Nevertheless, these partial attributions based on relative intensities point out that shared fluorine atoms have the lowest isotropic chemical shifts when the highest ones are for "free" fluorine atoms.

2. Superposition Model Applied to Fluoroaluminates. 2.1. Presentation of the Model. This model was proposed by B. Bureau et al.[8] for ionic fluorides. The ^{19}F isotropic chemical shift is considered as a sum of one constant diamagnetic term and several paramagnetic contributions from the neighboring M = Al, Ca, Ba cations. The calculation of δ_{iso} can be performed using the main formula of B. Bureau et al.: [8]

$$\delta_{iso/C_6F_6} = -127.1 - \sum \sigma_l \quad \text{with } \sigma_l = \sigma_{l_0} \exp[-\alpha_l(d - d_0)]$$

d_0 is the characteristic F−M distance which is taken equal to the bond length in the related basic fluoride (AlF_3, CaF_2, or BaF_2). σ_{l_0} is the parameter which determines the order of magnitude of the cationic paramagnetic contribution to the shielding and was deduced from measurements in the related basic fluoride where $\delta_{iso/C_6F_6} = -127.1 - n\sigma_{l_0}$ (n is the coordination number of the fluorine atom). For Al, Ca, and Ba whose atomic radial wave functions are known, α_l was deduced from the behavior of the cation isotropic paramagnetic contribution $\bar{\sigma}^p$ (see formula in appendix A of B. Bureau et al.[8]) calculated for several d distances on the basis of Ramsey's theory[9] with molecular orbitals obtained by Löwdin's orthogonalization method.[10]

Table 4. α_l (Å^{-1}), d_0 (Å), and σ_{l_0} (ppm) Parameters[8] and Comparison between Calculated and Experimental δ_{iso} Values (ppm) for Basic Fluorides

basic fluorides	α_l	d_0	σ_{l_0}	$\delta_{iso,cal}$	$\delta_{iso,exp}$
AlF_3	3.521	1.797	−61.0	−5	−5
CaF_2	2.976	2.366	−46.3	58	58
BaF_2	2.736	2.685	−70.0	153	153

The starting parameters we used in our calculations are those defined by Bureau et al.[8] They are gathered in Table 4. The last step, using the model, is to define the number of neighboring cations M whose contributions have to be taken into account. B. Bureau et al. chose the first cationic coordination sphere for the basic fluorides, and nearest and next nearest cations for compounds with two different cations. In the present work, the coordination spheres are not simple to define due to the low symmetry of the studied phases. For the calculation of δ_{iso} values, we decided to consider only atoms included in a sphere of 3.5 Å radius since for larger distances the cationic contributions become negligible.

The values obtained with this model are compared with the experimental results for CaF_2-AlF_3 and BaF_2-AlF_3 binary systems. The calculated and experimental isotropic chemical shifts are then paired, having regard for the first attribution based on the relative intensities, in order to minimize the difference:

$$\Delta\delta_{iso} = \delta_{iso,exp} - \delta_{iso,cal}$$

These attributions, referred hereafter as "initial attributions", are summarized in Tables 1−3. A comparison between calculated and experimental values is shown in Figure 6.

A linear regression provides the following result: $\delta_{iso,cal} = 1.207\delta_{iso,exp}$ with a correlation coefficient equal to 0.843. On the whole, the calculated values are overestimated. The RMS deviation is 25 ppm, and the maximum difference between measured and calculated δ_{iso} values reaches 80 ppm. Although the model has simplicity, the agreement is quite satisfactory.

However, Figure 6 shows two sets of points which follow different trends, evidenced by the two distinct linear regressions. They correspond to experimental δ_{iso} values above and below 100 ppm. Moreover, according to the initial attributions, the former group gathers all the "free" fluorine atoms related to barium. This seems to indicate that "free" fluorine atoms may have a different behavior from the shared and unshared ones, in the BaF_2-AlF_3 binary.

2.2. Improvement of the Phenomenological Parameters. In order to obtain a better agreement between the experi-

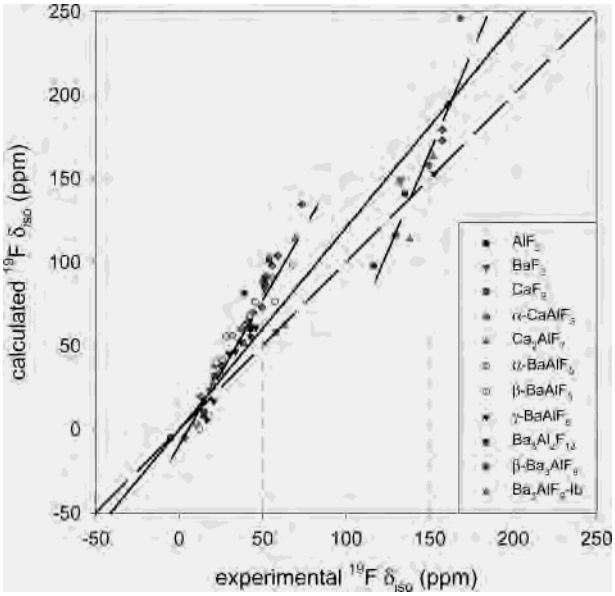

Figure 6. Isotropic chemical shift values calculated with phenomenological parameters defined by B. Bureau et al.[8] versus experimental ones. The linear regression and the $\delta_{iso,calc} = \delta_{iso,exp}$ curves correspond to a solid line and a dashed line, respectively, whereas the two distinct linear regressions related to experimental δ_{iso} values above and below 100 ppm are symbolized by long dashed lines.

Table 5. Refined α_l (Å^{-1}), d_0 (Å), and σ_{l_0} (ppm) Parameters and Comparison between Calculated and Experimental δ_{iso} Values (ppm) for Basic Fluorides

basic fluorides	α_l	d_0	σ_{l_0}	$\delta_{iso,cal}$	$\delta_{iso,exp}$
AlF_3	1.737	1.773	−63.1	−6	−5
CaF_2	3.303	2.353	−46.2	50	58
BaF_2 for $F_{s,u}$	2.125	2.660	−55.9		
BaF_2 for F_f	1.517	2.710	−67.6	154	153

mental and calculated values, a minimization of the sum of squares of the deviations between the two sets of values is searched through the optimization of the parameter sets (α_l, d_0, and σ_{l_0}) for each cation:

$$S = \sum(\delta_{iso,cal} - \delta_{iso,exp})^2$$

All values of Tables 1−4 are included in this calculation.

The best result is obtained with four sets of parameters instead of three. Whereas a single parameter set is sufficient for calcium and aluminum ions, two sets are needed for barium: one set related to the "free" fluorine atoms and a second one related to the other fluorine atoms. The parameter values for the four sets are gathered in Table 5.

New attributions of the NMR lines, named hereafter "final attributions", are then performed with respect for the first attribution based on the relative intensities. The final attributions are collected in Tables 1−3. The comparison between the new calculated values and the experimental ones is shown in Figure 7. A linear regression is performed and provides $\delta_{iso,cal} = 0.996\delta_{iso,exp}$ with a correlation coefficient equal to 0.981. The RMS deviation is 6 ppm, and the maximum difference between measured and calculated values is less than 20 ppm (Tables 1−3 and 5) for a chemical shift range of 175 ppm.

Due to the parameter variations and to be sure that the coordination sphere at 3.5 Å is still satisfactory, two tests

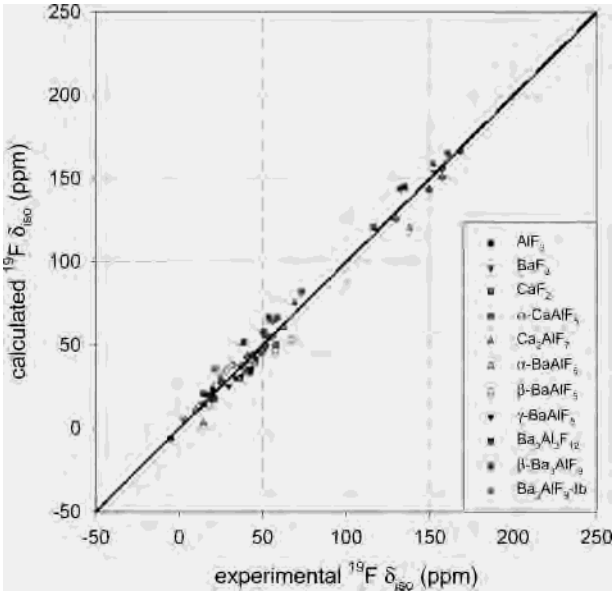

Figure 7. Isotropic chemical shift values calculated with refined phenomenological parameters versus experimental ones. The linear regression (solid line) and the $\delta_{iso,calc} = \delta_{iso,exp}$ curves (dashed line) are nearly superimposed.

Table 6. Refined α_l (Å^{-1}), d_0 (Å), and σ_{l_0} (ppm) Parameters for 4.0 and 4.5 Å Radius Coordination Spheres

sphere radius	basic fluorides	α_l	d_0 (Å)	σ_{l_0}
4.0 Å	AlF_3	1.618	1.803	−57.4
	CaF_2	3.002	2.342	−47.9
	BaF_2 for $F_{s,u}$	2.287	2.623	−61.8
	BaF_2 for F_f	1.196	2.721	−66.1
4.5 Å	AlF_3	1.330	1.785	−50.9
	CaF_2	2.150	2.354	−46.7
	BaF_2 for $F_{s,u}$	2.097	2.637	−59.2
	BaF_2 for F_f	1.462	2.711	−64.5

have been performed with sphere radii of 4.0 and 4.5 Å as limits for the fluorine coordination shells. The parameter values for those two coordination spheres are summarized in Table 6. On one hand, a slightly better correlation between experimental and calculated values is reached, as the RMS deviation is equal to 6 and 5 ppm, respectively. On the other hand, the parameter sets lead to cationic contributions which are nearly identical to those obtained for the 3.5 Å radius coordination sphere, but the data collection for modeling is more time-consuming. So, the four sets of parameters issued from the refinement with the coordination sphere at 3.5 Å are kept for δ_{iso} calculations.

Discussion

1. Line Attribution. In CaF_2-AlF_3 binary system, initial and final attributions are the same (Table 1). For Ca_2AlF_7 compound, F4 and F5 that are both assigned to line 2 have very close δ_{iso} calculated values, at 24 and 22 ppm, respectively. The line attributions are ascertained for all fluorine atoms.

For the α-$BaAlF_5$ form also, there is no change between initial and final attributions (Table 2). However, assignation of F4 to line 2 and of F3 to line 3 is not certain as the difference between their δ_{iso} calculated values is very small, within the RMS deviation of 6 ppm: attribution of F3 to line 2 and of F4 to line 3 is also possible. F1 and F2 have their

δ_{iso} values calculated at 49 and 55 ppm, respectively, and their line attributions may also be inverted. So line 1 is attributed to the shared fluorine F5 whereas lines 2−5 are assigned to the unshared ones.

Initial and final attributions are inverted for F9 and F6 in β-$BaAlF_5$. However, considering that their δ_{iso} calculated values are 38 and 34 ppm, respectively, that F7 is calculated between at 37 ppm, and that the RMS deviation is 6 ppm, the line assignation for F6, F7, and F9 is not definite. For similar reasons, F7, F6, and F4 may be exchanged too. F1 and F5, the two shared fluorine atoms, have their δ_{iso} values calculated at 13 and 14 ppm, respectively, and their line attributions may also be inverted. So, for this compound, lines 1 and 2, which have the smallest δ_{iso} values, are each attributed to a shared fluorine atom. The remaining lines are assigned to the unshared fluorine atoms, and the attributions are ascertained for F3 and F8.

For γ-$BaAlF_5$, initial and final attributions are similar only for F10, F4, and F3, but the line assignation is only sure for F3 (Table 2). For all other fluorine atoms, exchanges may be done since the differences between δ_{iso} calculated values are within the 6 ppm RMS deviation. It implies that for lines 4−8, the fluorine atoms are of unshared type whereas for lines 1−3 the kinds of fluorine environment are uncertain.

Initial and final attributions are analogous for $Ba_3Al_2F_{12}$ compound (Table 3). As F8 δ_{iso} calculated value is between those obtained for F1 and F2, it is also possible to assign F8 to line 1 and both F1 and F2 to line 2. F6 and F7 have their δ_{iso} values calculated at 58 and 52 ppm, respectively, so their line assignation is not confident. Consequently, lines 1 and 2 may be attributed indiscriminately to two shared fluorine atoms or one unshared fluorine atom. On the contrary, lines 3−5 are attributed without any doubt to unshared fluorine atoms and lines 6 and 7 to "free" ones.

There is no change between initial and final attributions for Ba_3AlF_9-Ib (Table 3), and all assignments are certain, due to the two different multiplicities.

For β-Ba_3AlF_9, initial and final attributions are similar only for nine fluorine atoms (Table 3). For F4, F10, F8, F6, F11, F9, and F12, exchanges may be done since the differences between δ_{iso} calculated values are within the RMS deviation. F2 and F5 δ_{iso} values are calculated at 64 and 66 ppm, respectively, and their line attributions may also be inverted. It is the same for F13 and F14 (δ_{iso} values calculated at 151 and 156 ppm, respectively), and for F15 and F16 (δ_{iso} values calculated at 164 and 166 ppm, respectively). On the contrary, F13 and F18, whose δ_{iso} values are calculated at 143 and 144 ppm, respectively, have their line attributions assured as F13 multiplicity is twice the F18 one. Consequently, lines 1−10 are attributed to the unshared fluorine atoms and lines 11−16 to the "free" ones. Moreover, the line assignments to a precise fluorine site are certain for F1, F3, F7, and F17−F19.

The line attributions are modified for 19 of the fluorine sites when the refined parameters are used. As RMS deviation is then nearly divided by 4, the number of unambiguous assignations increases from 15 to 27. Moreover, it is now possible to attribute a kind of fluorine environment to each line, except for 3 lines of γ-$BaAlF_5$ and 2 lines of $Ba_3Al_2F_{12}$.

2. Comparison with Previous Studies. Three of the compounds were already studied by Kiczenski et al.,[7] and a line attribution based on the fluorine first and second cationic shells was proposed. The same line attributions are obtained with our method for α-$CaAlF_5$ and Ca_2AlF_7, whereas agreement is only obtained for the line with the lowest δ_{iso} value (attributed to a shared fluorine atom) for α-$BaAlF_5$. The four remaining fluorine sites have one Al and a varying number of Ba as nearest neighbors. Considering that adding Ba neighbors shifts the line position to higher frequencies, lines 2 and 3 are assigned to F1 and F2, respectively, lines 4 and 5 to F3 and F4 in Kiczenski's study. Using the model with refined parameters, lines 4 and 5 are attributed to F1 and F2, respectively. This discrepancy is mostly due to the fact that, for those two fluorine atoms, the smallest Ba−F distance is lower than for F3 and F4. It implies that the calculated barium contribution to the fluorine shielding is higher in this case than for F3 and F4. This points out that the major advantage of the superposition model is to take into account distance effects quantitatively.

3. Interpretation of the Phenomenological Parameter Modifications. A comparison between initial (Table 4) and refined (Table 5) parameters (α_l, d_0, and σ_{l_0}) of the superposition model shows that the characteristic F−M distances d_0 have small variations and remain consistent with the fluorine−cation distances in the basic fluorides. σ_{l_0} values are also almost unchanged, except for Ba in shared and unshared fluorine environments. This means that the paramagnetic contribution of the cations determined in basic fluorides can be successfully used in more complex structures.

The most sensitive parameter is α_l, which describes the behavior of the paramagnetic contribution with the F−M distance. In order to understand more precisely the meaning of this parameter, the curves representing σ_l versus $d - d_0$ for the initial and final parameter sets are plotted in Figure 8 for each cation. The important point to notice is that, contrary to B. Bureau who determines α_l from calculations,[8] this parameter is now deduced from a large range of $d - d_0$ values as shown in Figure 8.

In the case of F−Ca bonds, the two curves are almost identical; i.e., there are only small differences between initial and refined parameters. The paramagnetic contributions are nearly the same with both parameter sets. The initial model established for purely ionic fluorides is a very good approximation.

For Al and Ba, the curves corresponding to the model with refined parameters slightly differ from those of the initial one. This may be correlated with deviation from the purely ionic model for F−Al and F−Ba bonds.

Actually, it is well-known that every heteronuclear bond has both covalent and ionic characters. It is possible to evaluate the partial ionic charges for the atoms in AlF_3, CaF_2, and BaF_2 compounds using Mulliken atomic electronega-

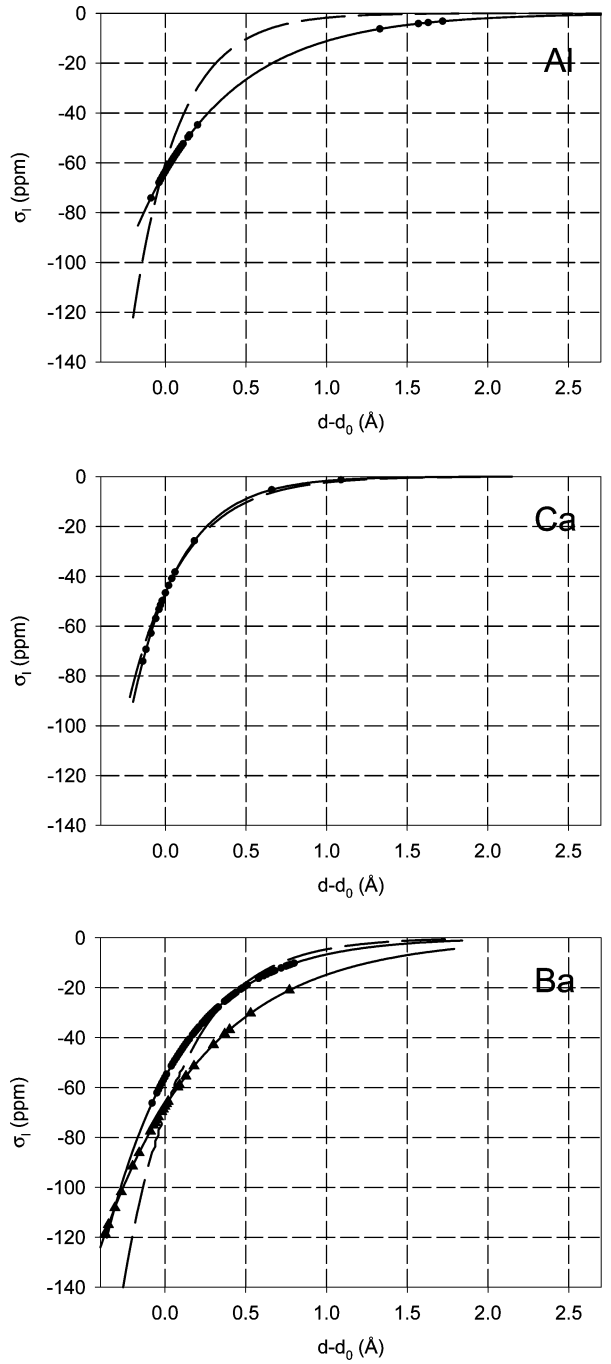

Figure 8. Paramagnetic contributions calculated with initial (- - -) and final (—) parameter sets for Al (top), Ca (middle), and Ba (bottom). Symbols are related to experimental ($d - d_0$) values. For barium, experimental ($d - d_0$) values for $F_{s,u}$—Ba and F_f—Ba bonds are distinguished by ● and ▲ symbols, respectively.

tivities.[30] For each atom, the electronegativity χ can be determined using the following formula:

$$\chi = a + b\delta$$

In this equation, a is the inherent Mulliken electronegativity, b the charge coefficient, and δ the partial ionic charge.

Calculation of a and b for each atom is performed according to the method proposed by S. T. Bratsch.[30] The

(30) Bratsch, S. T. *J. Chem. Educ.* **1988**, *65*, 34−41.

Table 7. Inherent Mulliken Electronegativities a, Charge Coefficients b, and Polarizabilities (10^{-30} C·m²·V^{-1}) for F, Ba, Ca, and Al Atoms

atom	a	b	polarizability
F	15.30	17.81	0.6
Ba	2.79	3.93	44.2
Ca	3.29	4.48	25
Al	5.61	6.12	7.57

Table 8. Partial Ionic Charges for F−Al, F−Ca, and F−Ba Bonds

	partial ionic charge	
compound	F	metal
AlF_3	−0.268	0.804
CaF_2	−0.448	0.896
BaF_2	−0.487	0.974

percentage of s orbital is 100/G, with G the atom group number. The resulting values are listed in Table 7.

When atoms are involved in a molecule or a crystal, their electronegativities come up to a common molecular electronegativity. It is then possible to determine the partial ionic charges for F−metal bonds in AlF_3, BaF_2, and CaF_2 compounds. These results are gathered in Table 8.

The aluminum atom has the smallest partial ionic charge, so the F−Al bond has the highest covalent character. In agreement with the smallest difference between inherent Mulliken electronegativities of Al and F (Table 7), the fact that the α_l value decreases from 3.5 for the purely ionic model (Table 4) to 1.7 after refinement (Table 5) may be related to the slightly covalent character of the F−Al bond. In other words, the orbital overlap between F and Al is larger than in a purely ionic model. In contrast, the covalent character of the F−Ba and F−Ca bonds is small, and the variations of α_l values after refinement for both atoms are less significant than for Al.

However, the covalent character of a F−metal bond is not sufficient to explain the use of two parameter sets for barium in the model with refined parameters. For $F_{s,u}$—Ba, where F is shared or unshared, the α_l value after refinement is not far from the initial one. This behavior is quite similar to the F−Ca one. On the contrary, for F_f—Ba bonds, the evolution of α_l after refinement is quite different. This may be tentatively related with the high polarizability of the barium atom. The polarizability values for the three atoms Ba, Ca, and Al[31] are compared in Table 7. Its high polarizability implies that Ba is more sensitive to the electric charges of the surrounding atoms. In the case of the $F_{s,u}$—Ba bond, the fluorine atom has at least one aluminum as nearest neighbor. So, in absolute values, its partial ionic charge is smaller than for "free" fluorine atoms in F_f—Ba bonds. This may result in a larger overlap between F_f and Ba orbitals than for $F_{s,u}$ and Ba ones, explaining the reduction of α_l parameter after refinement.

4. Validation of the Refined Parameter Sets on α-BaCaAlF$_7$. The refined parameter sets were applied to α-BaCaAlF$_7$ which is described from isolated AlF_6^{3-} octahedra separated from each other by calcium, barium, and "free" fluorine anions.[15] α-BaCaAlF$_7$ crystallizes in the monoclinic

(31) *Handbook of chemistry and physics*, 74th ed.; CRC Press: Boca Raton, FL, 1993.

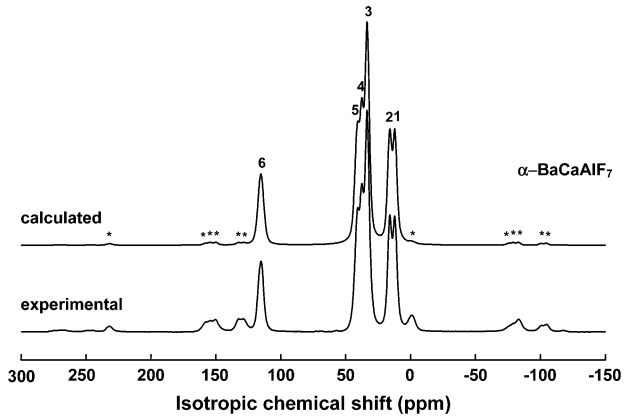

Figure 9. Calculated and experimental ^{19}F MAS NMR spectra of α-$BaCaAlF_7$ at 35 kHz. The spinning sidebands are located under the * symbols.

Table 9. Line Labels, Relative Intensities (%), and $\delta_{iso,exp}$ Values (ppm) As Deduced from NMR Spectrum Simulations, Line Attributions, $\delta_{iso,cal}$, and $\Delta\delta_{iso} = \delta_{iso,exp} - \delta_{iso,cal}$ after Refinement of the Superposition Model Parameters for α-$BaCaAlF_7$[a]

line	relative intensity (±2)	$\delta_{iso,exp}$ (±1)	final attribution site	$\delta_{iso,cal}$	$\Delta\delta_{iso}$
1	15	18	**F 2 (4g, u)**	**19**	**−1**
2	13	22	**F 3 (4g, u)**	**28**	**−6**
3	29	37	F 7 (4g, u)	35	2
			F 1 (4g, u)	35	2
4	15	41	F 5 (4g, u)	37	4
5	15	44	F 6 (4g, u)	41	3
6	13	112	**F 4 (4g, f)**	**100**	**12**

[a] s, u, and f indicate, respectively, shared, unshared, and "free" fluorine atoms. Unambiguous attributions are in boldface.

*P*2/*n* space group. Seven distinct fluorine sites are present in the structure, each with 4g multiplicity. Consequently, the experimental spectra are expected to show seven peaks. However, the recorded spectrum presented in Figure 9 shows only six peaks. Reconstruction of the experimental spectra at various spinning speeds is also obtained with six contributions. The data issued from the simulation of the spectrum recorded at 35 kHz (line labels, intensities, and δ_{iso} values) are collected in Table 9. Five of the six lines have relative intensities nearly around 14% so each one is assigned to one 4g-fluorine site. The relative intensity of the line 3 is twice that, about 29%, and is assigned to two 4g-fluorine sites.

The calculated values, obtained with the refined parameter sets, are in fine agreement with the experimental ones. Owing to the RMS deviation of 6 ppm, line attributions are certain for F2, F3, and F4.

5. Chemical Shift Ranges. From the final attributions performed with the refined parameter sets, it is also possible to define isotropic chemical shift ranges for the three fluorine types, in both CaF_2-AlF_3 and BaF_2-AlF_3 binary systems.

The shared fluorine atoms have the lowest isotropic chemical shifts, measured between 0 and 5 ppm for CaF_2-AlF_3 binary system, and between 10 and 30 ppm for BaF_2-AlF_3 binary system. Their cationic environments are close to the fluorine one in AlF_3 for which $\delta_{iso} = -5$ ppm.

On the contrary, the "free" fluorine atoms have the highest isotropic chemical shifts inside the studied binary systems. The "free" fluorine atom in Ca_2AlF_7 has an isotropic chemical shift measured at 63 ppm, near the δ_{iso} value of 58 ppm in CaF_2. For the BaF_2-AlF_3 binary system, the isotropic chemical shift range of the "free" fluorine atoms is measured between 105 and 170 ppm and includes BaF_2 for which $\delta_{iso} = 153$ ppm. Consequently, the isotropic chemical shift values for "free" fluorine atoms are found in the neighborhood of the δ_{iso} value of the corresponding cation−fluorine compound. This was already observed in $PbF_2-M^{II}F_2-M^{III}F_3$ (M^{II} = Ba, Zn; M^{III} = Ga, In) crystalline and glassy phases, where F_f δ_{iso} values were measured within the range of α- and β-PbF_2 values.[3]

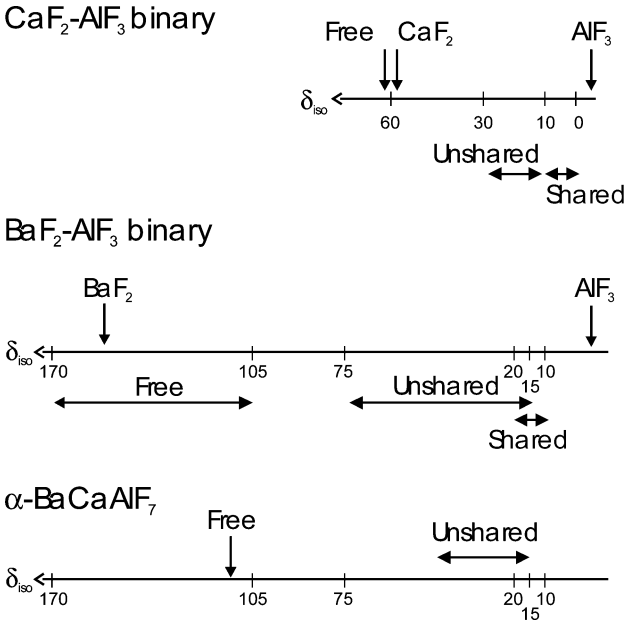

Figure 10. Isotropic chemical shift ranges of shared, unshared, and "free" fluorine atoms in CaF_2-AlF_3 and BaF_2-AlF_3 binary systems, and for α-$BaCaAlF_7$.

The unshared fluorine atoms, which have one aluminum and at least one calcium or barium atoms as nearest neighbors, have their isotropic chemical shifts between 10 and 30 ppm for the CaF_2-AlF_3 binary system, and between 15 and 75 ppm for the BaF_2-AlF_3 one. An overlap exists between the ranges of shared and unshared fluorine δ_{iso} values in BaF_2-AlF_3 binary system. However, there is no overlap between unshared and "free" fluorine isotropic chemical shifts for both binary systems.

The α-$BaCaAlF_7$ phase belongs to the $BaF_2-CaF_2-AlF_3$ ternary system. According to final line attributions (Table 9), the δ_{iso} values for the unshared fluorine atoms are situated between 15 and 45 ppm, which is consistent with the unshared fluorine ranges previously found for both binary systems. The "free" fluorine, with one barium and two Ca atoms as first neighbors, has an isotropic chemical shift measured at 112 ppm, between the δ_{iso} values measured for CaF_2 and BaF_2. Figure 10 presents the chemical shift ranges for the three kinds of fluorine atoms in the two binary systems and for α-$BaCaAlF_7$.

Now, the recorded spectrum of the β-$CaAlF_5$ form, presented in Figure 11, can be compared with the chemical shift ranges defined for the CaF_2-AlF_3 binary system. Four lines are resolved, and the spectrum reconstruction is

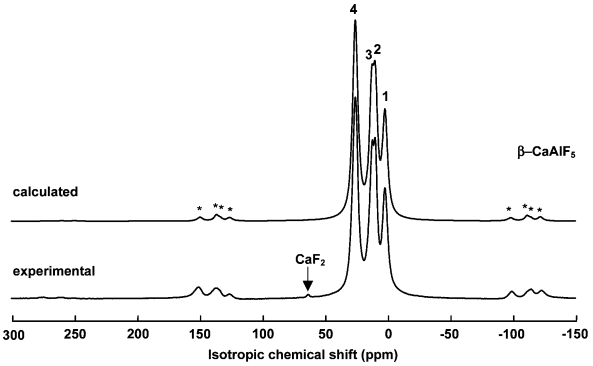

Figure 11. Calculated and experimental ^{19}F MAS NMR spectra of β-$CaAlF_5$ at 35 kHz. The spinning sidebands are located under the * symbols.

Table 10. Line Labels, Relative Intensities (%), and $\delta_{iso,exp}$ Values (ppm) As Deduced from NMR Spectrum Simulations and Fluorine Types for β-$CaAlF_5$[a]

line	relative intensity (±2%)	$\delta_{iso,exp}$ (±1 ppm)	fluorine type
1	20	2	s
2	19	10	u
3	21	13	u
4	41	26	u

[a] s and u indicate, respectively, shared and unshared fluorine atoms.

satisfactory with four contributions. The δ_{iso} values issued from the simulation at 35 kHz are collected in Table 10. Line 1 is located at 2 ppm, which indicates shared fluorine atoms. Lines 2 (10 ppm) and 3 (13 ppm) are both attributed to unshared fluorine atoms. Line 4 (26 ppm) is also positioned within the range defined for unshared fluorine atoms, and its relative intensity is nearly equal to 40%, twice that of the three other lines. It gives 20% of shared and 80% of unshared fluorine atoms, which indicates that β-$CaAlF_5$ structure is built up from isolated chains of AlF_6^{3-} octahedra. This is in agreement with J. Ravez et al. who found β-$CaAlF_5$ isotypic with $CaFeF_5$.[32] According to this hypothesis, the five fluorine sites have the same 4e multiplicity, and line 4 should be attributed to two 4e fluorine sites with very close isotropic chemical shifts.

Conclusions

High-speed MAS ^{19}F NMR spectra for 10 compounds, from BaF_2-AlF_3 and CaF_2-AlF_3 binary and $BaF_2-CaF_2-AlF_3$ ternary systems, were recorded at different spinning speeds and reconstructed using DMFIT software. This study led to the accurate determination of 77 ^{19}F isotropic chemical shifts between −5 and 170 ppm related to a large variety of site symmetries and fluorine−cation distances.

A first attribution of the NMR lines was performed using the superposition model and its phenomenological parameters for Al^{3+}, Ca^{2+}, and Ba^{2+} ions as initially proposed by B. Bureau et al.[8] This model was shown to be a good starting point. The RMS deviation between experimental and calculated values was found to be equal to 25 ppm.

Second, the phenomenological parameters of the model were refined. The NMR line assignment was improved, and the RMS deviation value was reduced to 6 ppm. A satisfactory reliability was then reached. One striking feature in this refinement procedure was the introduction of two sets of phenomenological parameters for Ba^{2+} according to whether the fluorine atoms are "free" or not. It was shown that the discrepancy between the starting and refined sets of parameters is connected with polarizability of the metal cations and covalency of the F−M bond, which are not taken explicitly into account in the model.

Then, the refined sets of parameters were successfully tested on α-$BaCaAlF_7$ which belongs to the $BaF_2-CaF_2-AlF_3$ ternary system.

Finally, from NMR line attributions, isotropic chemical shift ranges could be defined for the three kinds of fluorine environment encountered in the binary systems. Then, it is possible to infer fluorine surroundings from the NMR line positions when the crystalline structure is unknown. It supports the assumption that β-$CaAlF_5$ is isotypic with $CaFeF_5$.[32] Soon, the same procedure of identification of the fluorine types will be applied to glasses of the $BaF_2-CaF_2-AlF_3$ ternary system. Through the determination of the proportions of the three fluorine types from ^{19}F NMR spectra we should be able to describe the fluorine octahedron network in these fluoroaluminate glasses. Ab initio calculations of ^{19}F chemical shifts are also in progress for comparison.

Acknowledgment. We thank A. Le Bail and A.-M. Mercier, from the Laboratoire des Oxydes et Fluorures CNRS UMR 6010, who kindly supplied us with the three $BaAlF_5$ phases and M. Leblanc, from the same laboratory, for his careful reading of this manuscript.

IC049956R

(32) Ravez, J.; Hagenmuller, P. *Bull. Soc. Chim. Fr.* **1967**, *7*, 2545−2548.